NASA TECHNICAL MEMORANDUM

NASA TM X-2227

NASA TM X-2227

ANALYSIS OF OPTICAL COMPONENT MOVEMENT BY HOLOGRAPHIC INTERFEROMETRY

by John R. Williams and B. Nelson Norden

George C. Marshall Space Flight Center
Marshall Space Flight Center, Ala. 35812

NATIONAL AERONAUTICS AND SPACE ADMINISTRATION • WASHINGTON, D. C. • MARCH 1971

1. REPORT NO.	2. GOVERNMENT ACCESSION NO.	3. RECIPIENT'S CATALOG NO.
NASA TM X-2227		

4. TITLE AND SUBTITLE	5. REPORT DATE
Analysis of Optical Component Movement by Holographic Interferometry	March 1971
	6. PERFORMING ORGANIZATION CODE
7. AUTHOR(S)	8. PERFORMING ORGANIZATION REPORT #
John R. Williams and B. Nelson Norden	M-437
9. PERFORMING ORGANIZATION NAME AND ADDRESS	10. WORK UNIT NO.
George C. Marshall Space Flight Center Marshall Space Flight Center, Alabama 35812	11. CONTRACT OR GRANT NO.
	13. TYPE OF REPORT & PERIOD COVERED
12. SPONSORING AGENCY NAME AND ADDRESS	Technical Memorandum
National Aeronautics and Space Administration Washington, D. C.	14. SPONSORING AGENCY CODE

15. SUPPLEMENTARY NOTES

Prepared by the Space Sciences Laboratory
Science and Engineering Directorate

16. ABSTRACT

Several efforts are within NASA which are directed toward the eventual orbiting of a large (~3 meters) telescope. This type of endeavor generates many problems and questions which for the most part require state-of-the-art answers. One obvious question is: Do the mirror characteristics change while in orbit, and, if so, to what degree? This report presents a quick look at the application of holographic interferometry to mirror movement, since numerous parameters such as mount sag, mirror surface creep, etc., manifest themselves in the form of displacements. Both theoretical and experimental data are presented for simple mirror rotation with a theoretical extension to include three-dimensional translation.

17. KEY WORDS	18. DISTRIBUTION STATEMENT
	Unclassified - Unlimited

19. SECURITY CLASSIF. (of this report)	20. SECURITY CLASSIF. (of this page)	21. NO. OF PAGES	22. PRICE*
Unclassified	Unclassified	41	$3.00

*For sale by the National Technical Information Service, Springfield, Virginia 22151

Page Intentionally Left Blank

TABLE OF CONTENTS

LIST OF ILLUSTRATIONS

TECHNICAL MEMORANDUM X-

ANALYSIS OF OPTICAL COMPONENT MOVEMENT BY HOLOGRAPHIC INTERFEROMETRY

SUMMARY

Several efforts are within NASA which are directed toward the eventual orbiting of a large (~3 meters) telescope. This type of endeavor generates many problems and questions which for the most part require state-of-the-art answers. One obvious question is: Do the mirror characteristics change while in orbit, and, if so, to what degree? This report presents a quick look at the application of holographic interferometry to mirror movement, since numerous parameters such as mount sag, mirror surface creep, etc., manifest themselves in the form of displacements. Both theoretical and experimental data are presented for simple mirror rotation with a theoretical extension to include three-dimensional translation.

I. INTRODUCTION

With the development of wavefront reconstruction (holography), literally a third dimension was added to the science of interferometry. The hologram allows a tremendous amount of information to be "frozen in time" for later analysis or comparison. The latter is the case that has such a dramatic effect on interferometry; i.e., the ability to compare one wavefront at one point in time with another wavefront at some other point in time. With this capability, a holographic interferometer (Holometer) is sensitive to object movement or displacement.

In considering some of the many problems associated with orbiting a large astronomical telescope, one immediately realizes that the definition of the optical surface is of overwhelming importance. This surface may be affected and/or changed by numerous sources such as mount sag, mirror material creep or flow, radiation, contamination[1], etc. Most of these sources are displayed by a mirror surface displacement, so the ability to detect such a displacement and to determine its direction(s) and magnitude(s) would be extremely useful.

---

1. A unique holographic interferometer is being used to study this effect and will be reported at the annual meeting of the Optical Society of America, September 29 through October 2, 1970, in Hollywood, Florida.

II. THEORETICAL FRINGE ANALYSIS

The following fringe analysis follows that by Haines and Hildebrand [1,2] and can be divided into three conditional areas. These areas are: (a) the case in which the fringes are on or very close to the object, (b) the case in which the fringes form at least several thousand wavelengths from the object, and (c) the general case in which the fringes are allowed to form at any distance from the object.

In case (a) the term "very close" refers to distances of a few thousand wavelengths or less. To produce this case, the object has undergone a rotation or translation along the line of sight only. This, of course, represents the easiest case to analyze and understand. The necessary and sufficient condition of object rotation for this case is well known from the theory of interferometry. Figure 1 illustrates this case. The coordinate system is attached to the point about which the object surface has been rotated. The surface has been rotated by an angle a. With the line of observation along the z axis and an angle β between the surface and the source, the path difference for any point on x is given by

$$\Delta\mathcal{L} = x\, a\, (1 + \sin\beta) \quad . \tag{1}$$

From this it is obvious that the radiation from the image and from the object differ only by a linear phase δ where,

$$\delta = \frac{2\pi}{\lambda}\, x\, a\, (1 + \sin\beta) \quad . \tag{2}$$

In this case, parallel fringes will form on or very near the surface and parallel to the axis of rotation. Equations (1) and (2) describe the case where the rotation is about the y-axis. The distance D between fringes near the point of observation is

$$D = \frac{\lambda}{a}\, (1 + \sin\beta)^{-1} \quad . \tag{3}$$

Thus, the degree of rotation may be found by measuring D and solving equation (3) for a.

If a small distance along the line of observation exists between the object and image (still assuming rotation), then the fringes will form between the object and image and it will be virtually impossible to differentiate this case from that of pure rotation. However, this ambiguous situation does not exist when the object is examined from two different angles through the hologram. This is also true for cases b and c. It will become evident that, to eliminate this type of ambiguity, it is always necessary to view the object from two different angles.

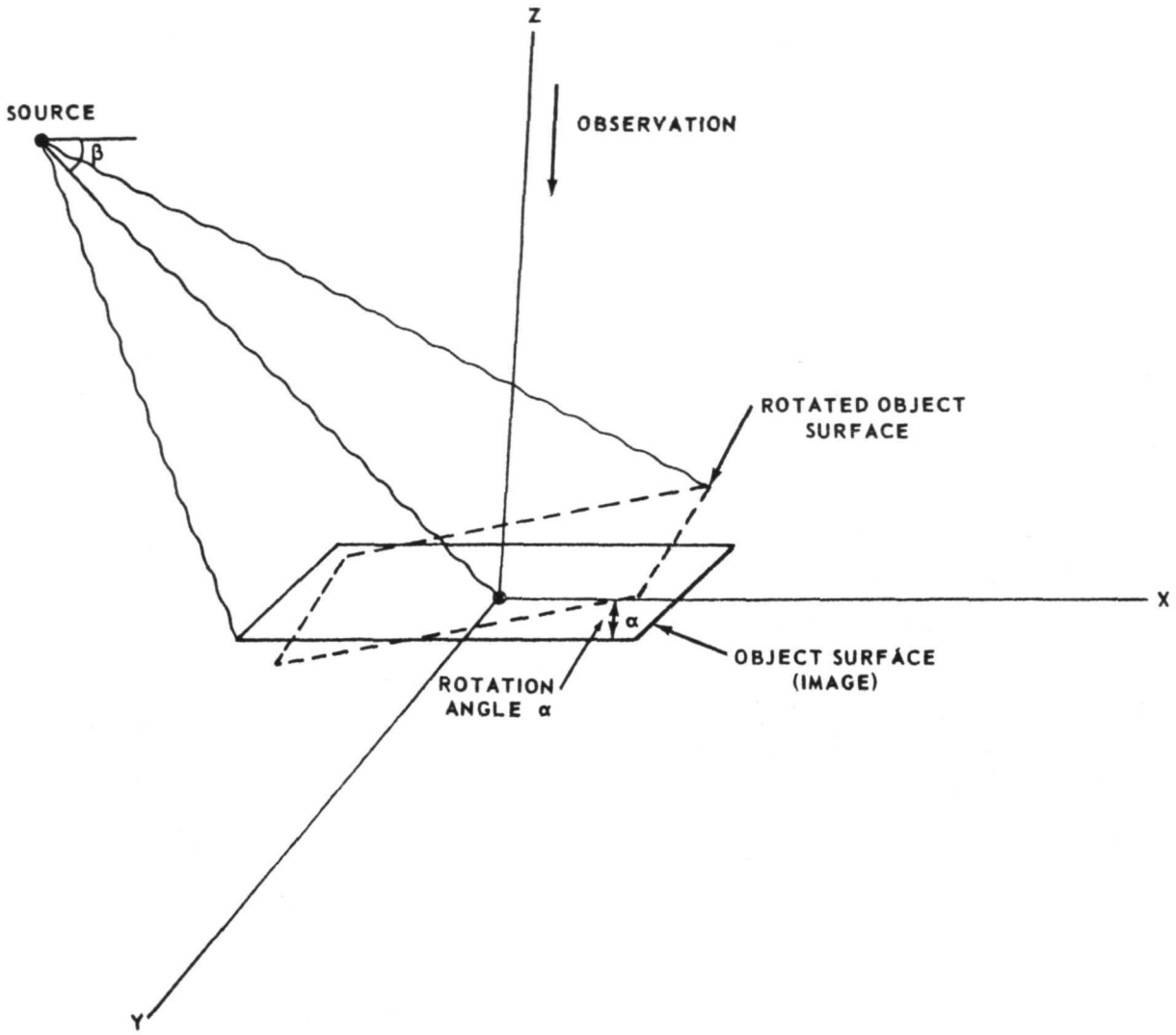

Figure 1. Object rotation coordinates.

In case b, the fringes form at least several thousand wavelengths from the object surface. The object surface is the small area about the point under consideration. In this more general case, one may have translation and rotation together or translation alone. For clarity, the object from which the holographic image was made is designated as object 1, and the object against which this image is to be compared is designated as object 2.

The Cartesian coordinate system is attached to the point on the surface to be observed. Let $f(x_1, y_1, z_1)$ be the complex reflectivity for the point x_1, y_1, z_1 on the object surface. Then, for a general illumination front $s(x_1, y_1, z_1)$ on the object, the light leaving the surface may be expressed as $f(x_1, y_1, z_1)\, s(x_1, y_1, z_1)$. It will be assumed that the illumination is of constant amplitude at the surface of the object and that it is generated

by a point source located at the coordinates x_o, y_o, z_o. Suppose that the object, object 2 in this instance, is a slightly rotated and translated facsimile of the image made from object 1. The rotations may be described in terms of Euler angles $\alpha, \beta,$ and γ as in Figure 2.

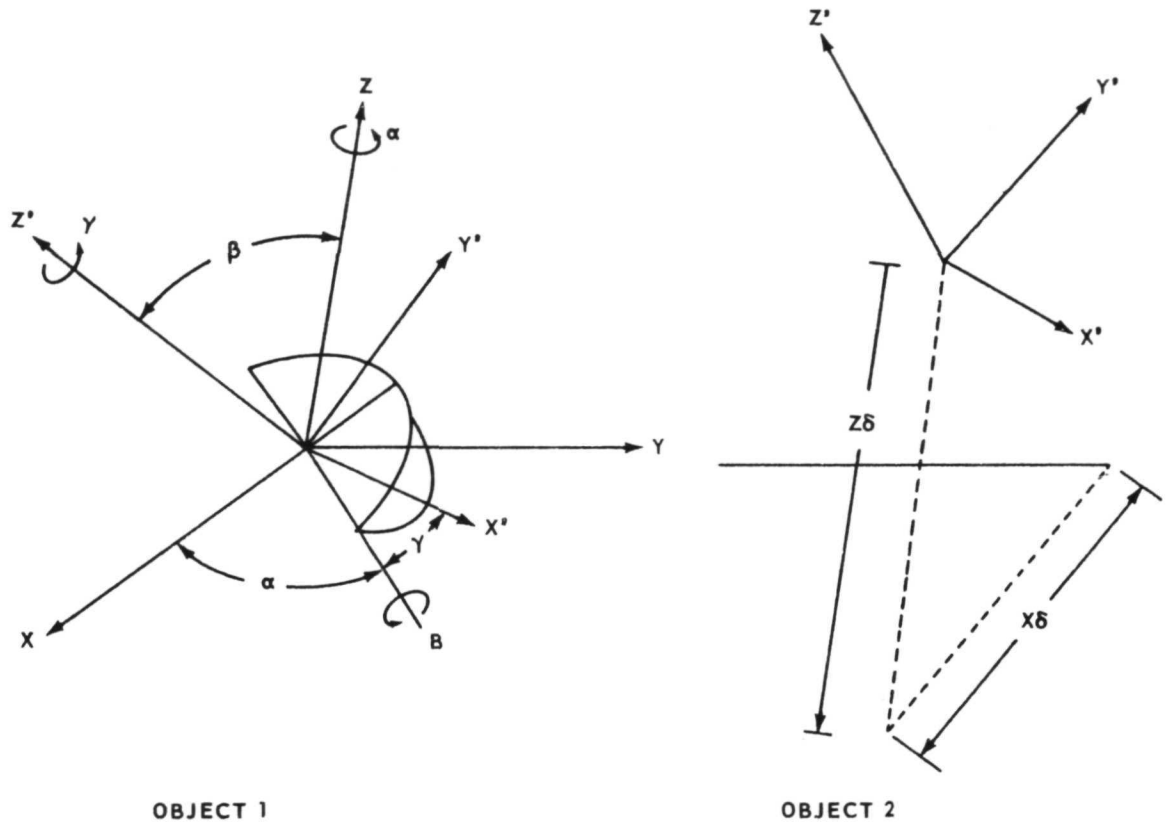

Figure 2. Coordinate transformation.

The translations may be designated by $x_g, y_g,$ and z_g. Euler angles relate the primed coordinates to the original coordinates by the Euler matrix

$$\begin{vmatrix} x' \\ y' \\ z' \end{vmatrix} = \begin{vmatrix} \cos\alpha\cos\gamma - \sin\alpha\cos\beta\sin\gamma & -\cos\alpha\cos\beta\sin\gamma - \sin\alpha\cos\gamma & \sin\beta\sin\gamma \\ \sin\alpha\cos\beta\cos\gamma + \cos\alpha\sin\gamma & \cos\alpha\cos\beta\cos\gamma - \sin\alpha\sin\gamma & -\sin\beta\cos\gamma \\ \sin\alpha\sin\beta & \cos\alpha\sin\beta & \cos\beta \end{vmatrix} \begin{vmatrix} x \\ y \\ z \end{vmatrix} . \quad (4)$$

For small rotations, $(\alpha + \gamma)$ and β are small, and this relationship becomes

$$\begin{vmatrix} x' \\ y' \\ z' \end{vmatrix} = \begin{vmatrix} 1 & -\gamma - \alpha & \beta \sin \gamma \\ \alpha + \gamma & 1 & -\beta \cos \gamma \\ \beta \sin \alpha & \beta \cos \alpha & 1 \end{vmatrix} \begin{vmatrix} x \\ y \\ z \end{vmatrix} . \tag{5}$$

In shorthand notation, these matrices may be written as

$$\left| X' \right| = \left| E_{X'X} \right| \left| X \right| . \tag{6}$$

When translations are also considered, equation (6) must be revised.

$$\left| X' \right| = \left| E_{X'X} \right| \left(\left| X \right| - \left| T \right| \right) \tag{7}$$

where

$$\left| T \right| = \begin{vmatrix} x_g \\ y_g \\ z_g \end{vmatrix} . \tag{8}$$

The transmission function of object 2 is designated by $f(x_1', y_1', z_1')$ where the primed coordinates are related to the unprimed coordinates by equation (7). The problem reduces to a comparison of the radiation at some general observation point x, y, z as it arrives from object 1 (which is actually the image generated by the hologram) and from object 2.

The diffraction pattern at this point from the image or object 1 may be approximated for large x, y, z, as

If all rotations and translations are so small that second-order terms involving these quantities may be neglected, equation (16) simplifies to:

$$\sum_i (d_i)^2 = (x - x_1')^2 + (y + y_1')^2 + (z - z_1')^2 + 2x_1' \left[x_g + y(\alpha + \gamma) - z\beta \sin\gamma \right]$$

$$+ 2y_1' \left[y_g - x(\alpha + \gamma) + z\beta\cos\gamma \right] + 2z_1' \left[z_g - x\beta \sin\alpha - y\beta\cos\alpha \right]$$

$$- 2 (x_g x + y_g y + z_g z) \quad . \tag{17}$$

Let $R = (x^2 + y^2 + z^2)^{1/2}$. Then the previous assumption that R is much larger than all other parameters allows the square root of equation (17) to be approximated by the first two terms in its binomial expansion.

$$\left[\sum_i (d_i)^2 \right]^{1/2} = R - \frac{xx_1' + yy_1' + zz_1'}{R} + \frac{x_1'^2 + y_1'^2 + z_1'^2}{2R} + \frac{x_1' \left[x_g + y(\alpha + \gamma) - z\beta\sin\gamma \right]}{R}$$

$$+ \frac{y_1' \left[y_g - x(\alpha + \gamma) + z\beta\cos\gamma \right]}{R} + \frac{z_1' \left[z_g - x\beta\sin\alpha - y\beta\cos\alpha \right]}{R}$$

$$- \frac{x_g x + y_g y + z_g z}{R} - \frac{(x_1' x + y_1' y + z_1' z)(x x_g + y y_g + z z_g)}{R^3} \quad . \tag{18}$$

Similarly, the other summations can be evaluated:

$$\left[\sum_i (c_i)^2 \right]^{1/2} = R_0 - \frac{x_0 x_1' + y_0 y_1' + z_0 z_1'}{R_0} + \frac{x_1'^2 + y_1'^2 + z_1'^2}{2R_0} + \frac{x_1' \left[x_g + y_0(\alpha + \gamma) - z_0 \beta \sin\gamma \right]}{R_0}$$

$$+ \frac{y_1' \left[y_g - x_0(\alpha + \gamma) + z_0 \beta\cos\gamma \right]}{R_0} + \frac{z_1' \left[z_g - x_0 \beta \sin\alpha - y_0 \beta\cos\alpha \right]}{R_0}$$

$$- \frac{x_g x_0 + y_g y_0 + z_g z_0}{R_0} - \frac{(x_1' x_0 + y_1' y_0 + z_1' z_0)(x_0 x_g + y_0 y_g + z_0 z_g)}{R_0^3} \tag{19}$$

where

$$R_0 = (x_0^2 + y_0^2 + z_0^2)^{1/2}$$

$$\left[\sum_i (a_i)^2\right]^{1/2} = R_0 - \frac{x_0\, x_1 + y_0\, y_1 + z_0\, z_1}{R_0} + \frac{x_1^2 + y_1^2 + z_1^2}{2R_0} \qquad (20)$$

$$\left[\sum_i (b_i)^2\right]^{1/2} = R - \frac{xx_1 + yy_1 + zz_1}{R} + \frac{x_1^2 + y_1^2 + z_1^2}{2R} \quad . \qquad (21)$$

The general expression

$$R_n = \frac{x_n x + y_n y + z_n z}{R_n} + \frac{x^2 + y^2 + z^2}{2R_n}$$

may be written as

$$\frac{1}{R_n}\left[(x_n - x)^2 + (y_n - y)^2 + (z_n - z)^2\right] \quad .$$

With this, equation (9) for U_1 becomes

$$U_1 = \iiint f(x_1, y_1, z_1) \exp\left\{\frac{-2\pi i}{\lambda}\left[\frac{(x_0 - x)^2 + (y_0 - y)^2 + (z_0 - z)^2}{R_0} \pm \frac{(x - x_1)^2 + (y - y_1)^2 + (z - z_1)^2}{R}\right]\right\} dx_1, dy_1, dz_1 \qquad (22)$$

and

$$U_2 = \iiint f(x_1', y_1', z_1') \exp\left\{\frac{-2\pi i}{\lambda}\left[\frac{(x_0 - x_1')^2 + (y_0 - y_1')^2 + (z_0 - z_1')^2}{R_0}\right.\right.$$

$$\left.\left. \pm \frac{(x - x_1')^2 + (y - y_1')^2 + (z - z_1')^2}{R}\right]\right\}$$

$$\times \exp\left\{-\frac{-2\pi i}{\lambda}\left[x_1'\left(\frac{x_g + y_0(\alpha + \gamma) - z_0\,\beta \sin\gamma}{R_0} - \frac{x_0(x_0\,x_g + y_0\,y_g + z_0\,z_g)}{R_0^3}\right.\right.\right.$$

$$\left.\left.\left. \pm \frac{x_g + y(\alpha + \gamma) - z\,\beta \sin\gamma}{R} \mp \frac{x(xx_g + yy_g + zz_g)}{R^3}\right)\right]\right.$$

$$+ y_1'\left[\frac{y_g - x_0(\alpha + \gamma) + z_0\,\beta\cos\gamma}{R_0} - \frac{y_0(x_0\,x_g + y_0\,y_g + z_0\,z_g)}{R_0^3}\right.$$

$$\left. \pm \frac{y_g - x(\alpha + \gamma) + 2\beta\cos\gamma}{R} \mp \frac{y(xx_g + yy_g + zz_g)}{R^3}\right]$$

$$+ z_1'\left[\frac{z_g - x_0\,\beta\sin\alpha - y\,\beta\cos\alpha}{R_0} - \frac{z_0(x_0\,x_g + y_0\,y_g + z_0\,z_g)}{R_0^3}\right.$$

$$\left. \pm \frac{z_g - x\,\beta\sin\alpha - y\,\beta\cos\alpha}{R} \mp \frac{z(xx_g + yy_g + zz_g)}{R^3} - \frac{x_g\,x_0 + y_g\,y_0 + z_g\,z_0}{R_0}\right.$$

$$\left.\left. - \frac{x_g x + y_g y + z_g z}{R}\right]\right\} \qquad (23)$$

Inspection of equations (22) and (23) reveals that the summation of the two may be expressed as:

$$U_1 + U_2 = \iiint \tilde{f}(x_1, y_1, z_1)\, dx_1, dy_1, dz_1$$

$$+ \exp(i\xi) \iiint \tilde{f}(x_1, y_1, z_1) \exp\left[-i(w_x x_1 + w_y y_1 + w_z z_1)\right] dx_1, dy_1, dz_1 \qquad (24)$$

where

$$\tilde{f}(x_1, y_1, z_1) = f(x_1, y_1, z_1) \exp\left\{ \frac{-2\pi i}{\lambda} \left[\frac{(x_0 - x_1)^2 + (y_0 - y_1)^2 + (z_0 - z_1)^2}{R_0} \right.\right.$$

$$\left.\left. \pm \frac{(x - x_1)^2 + (y - y_1)^2 + (z - z_1)^2}{R} \right] \right\} \qquad (25)$$

$$\xi = \frac{2\pi}{\lambda} \left[\frac{x_g x_0 + y_g y_0 + z_g z_0}{R_0} \pm \frac{x_g x + y_g y + z_g z}{R} \right] \qquad (26)$$

$$w_x = \frac{2\pi}{\lambda} \left[\frac{x_g + y_0(\alpha + \gamma) - z_0 \beta \sin\gamma}{R_0} - \frac{x_0(x_0 x_g + y_0 y_g + z_0 z_g)}{R_0^3} \right.$$

$$\left. \pm \frac{x_g + y(\alpha + \gamma) - z\beta \sin\gamma}{R} \mp \frac{x(x x_g + y y_g + z z_g)}{R^3} \right] \qquad (27)$$

$$w_y = \frac{2\pi}{\lambda} \left[\frac{y_g - x_0(\alpha + \gamma) + z_0 \beta \cos\gamma}{R_0} - \frac{y_0(x_0 x_g + y_0 y_g + z_0 z_g)}{R_0^3} \right.$$

$$\left. \pm \frac{y_g - x(\alpha + \gamma) + z\beta \cos\gamma}{R} \mp \frac{y(x x_g + y y_g + z z_g)}{R^3} \right] \qquad (28)$$

$$w_z = \frac{2\pi}{\lambda} \left[\frac{z_g - x_0 \beta \sin\alpha - y_0 \beta \cos\alpha}{R_0} - \frac{z_0(x_0 x_g + y_0 y_g + z_0 z_g)}{R_0^3} \right.$$

$$\left. \mp \frac{z_g - x\beta \sin\alpha - y\beta \cos\alpha}{R} \mp \frac{z(x x_g + y y_g + z z_g)}{R^3} \right] . \qquad (29)$$

Using Fourier Transform Theory, we may rewrite equation (24) as

$$U_1 + U_2 = F(o) + e^{i\xi} F(w_x, w_y, w_z) \tag{30}$$

where $F(o)$ is the value of the Fourier Transform at $w_x = w_y = w_z = 0$.

If $w_x = w_y = w_z = 0$ this expression represents the addition of two wavefronts, identical except for a linear phase term. This is the requirement for interference fringes to form. The spatial frequency of the fringes that form is determined by the linear phase term ξ which is invariant to a rotation of coordinates and may thus be written as

$$\xi = \frac{2\pi}{\lambda} \left[\frac{x_g x_{0\ell} + y_g y_{0\ell} + z_g z_{0\ell}}{R_0} \pm \frac{x_g x_\ell + y_g y_\ell + z_g z_\ell}{R_\ell} \right] \tag{31}$$

where the subscript ℓ refers to the coordinates system aligned along the R_ℓ vector. By differentiating ξ with respect to x_ℓ and y_ℓ, it is possible to evaluate x_g and y_g which are now displacements lateral to the R_ℓ vector (line-of-sight vector) using the relationships

$$x_g = \frac{\lambda R_\ell}{D_x} \tag{32}$$

$$y_g = \frac{\lambda R_\ell}{D_y} \tag{33}$$

where D_x and D_y are the interfringe spacings in the x_ℓ and y_ℓ directions. However, no equation results for z_g, and for that reason the fringe structure at some other point must be examined. Then all three translations x_g, y_g, and z_g in the original coordinate system may be determined.

Case 3 is a more general analysis than the two previous cases. The fringes are allowed to form at any distance from the object. This was not possible in the two previous cases since the Fresnel-Kirchkoff formula was not applicable. This analysis uses the theory of diffraction grating, and the results are identical to those for the other two cases with

their corresponding assumptions. A technique for such an analysis may be evolved by breaking the general three-dimensional object into a series of independent planes whose orientation is normal to some arbitrary axis. It is then possible to further break each individual plane into a series of x- and y-oriented sinusoidal gratings. Suppose, for example, that one such x-y plane through the object at distance z from the origin (Fig. 3) is represented by an infinite sum of gratings whose grating spacings in the x and y directions are $1/\nu$ and $1/\eta$. Then the x-y plane of the object can be represented by

$$f(x, y) = \sum_{\nu=-\nu}^{\infty} \sum_{\eta=-\nu}^{\infty} f_{\nu\eta} \exp(2\pi i \nu x + 2\pi i \eta y) \quad . \tag{34}$$

The propagation of each individual plane wave, radiating from each individual grating, is well understood from field theory. A plane wave given by $\exp(iax_1 + iby_1 + icz_1)$ at the origin results in a wavefront whose spatial distribution is $\exp(iax + iby + icz)$ at a point x, y, z where

$$a^2 + b^2 + c^2 = k^2 = \left(\frac{2\pi}{\lambda}\right)^2 \quad . \tag{35}$$

If all such plane waves from planes at all values of Z are summed at x, y, z, one then has a technique for finding the diffraction pattern at any point, even those close to the object. This is the technique to be used here. Results from the previous case will be used whenever applicable.

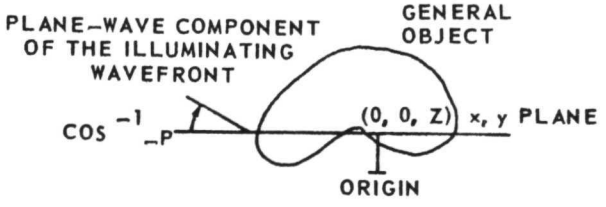

Figure 3. Decomposition of object into planes.

Let us suppose that the object plane of interest is illuminated by some general wavefront. This wavefront is not necessarily a plane wave, although certainly plane-wave illumination makes the analysis simpler. In general, the illuminating wavefront will be an infinite sum of plane waves, each having a direction cosine with the x axis at the x, y, Z plane denoted by p and a direction cosine in the y axis denoted by q. A plane wave of direction cosine p, striking a grating of spacing $1/\nu$, radiates a plane wave of direction cosine ϕ_x, where (Fig. 4)

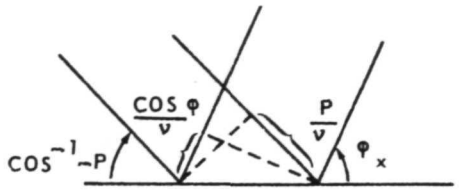

Figure 4. Grating geometry.

$$\cos \phi_x = p - \lambda\nu \quad . \tag{36}$$

Summing over all gratings in the xy plane of interest we can represent the light radiated from the object as

$$f(x, y, Z) = \sum_p \sum_q \sum_\nu \sum_\eta f_{\nu\eta} \exp \left[-ik(p - \lambda\nu)\lambda - ik(q - \lambda\eta)y\right] \quad . \tag{37}$$

The diffracted wavefront at any general field point x, y, z is then

$$U_Z(x, y, z) = \sum_p \sum_q \sum_\nu \sum_\eta f_{\nu\eta} \exp \left[-ik(p - \lambda\nu)x - ik(q - \lambda\eta) - ik(\ell - \lambda\mu)(z - Z)\right] \quad . \tag{38}$$

Since the wave equation holds everywhere, ℓ and μ are dependent on p, q, μ, and η through the relationship

$$\ell^2 + p^2 + q^2 = 1 \tag{39}$$

$$(p - \gamma\nu)^2 + (q - \lambda\eta)^2 + (\ell - \lambda\mu)^2 = 1 \quad . \tag{40}$$

A matrix notation is used, as was done in the previous case. Equation (38) may then be written as

$$U_Z(x, y, z) = \sum_p \sum_q \sum_\nu \sum_\eta f_{\nu\eta} \exp \left[ik \sum h_i\right] \tag{41}$$

where h_i is a general term in the matrix

$$\left|H\right| = \left|p - \lambda\nu \qquad q - \lambda\eta \qquad \ell - \lambda\mu\right| \left[\begin{vmatrix} x \\ y \\ z \end{vmatrix} - \begin{vmatrix} 0 \\ 0 \\ Z \end{vmatrix}\right] \quad . \tag{42}$$

In the conventional shorthand notation,

$$\left|H\right| = \left|p - \lambda\nu\right|^{T} (|X| - |Z|) \quad . \tag{43}$$

It is this diffracted wavefront that is actually generated by the hologram which is to be compared to a similar wavefront diffracted by the object in another position.

Consider the situation illustrated in Figure 5, in which the object is slightly translated and rotated about the origin. The diffracted wavefront at the field point x', y', z' may be written directly from equation (38)

$$U_Z'(x', y', z') = \sum_p \sum_q \sum_\nu \sum_\eta f_{\nu\eta} \exp\left[-ik(p' - \lambda\nu)k' - ik(q' - \lambda\eta)y' - ik(\ell - \lambda\mu)(z' - Z)\right] \tag{44}$$

The primed coordinates x', y', z' refer to the coordinate system of the rotated and translated object as in the previous case. The cosines p', q', ℓ' are now different from p, q, ℓ since they also refer to the rotated and translated coordinates of the objects. However, if the rotations and translations are very small compared to the distances to the illuminating source origin, p', q', and ℓ' may be approximated as $p+\Delta p, q+\Delta q$, and $\ell+\Delta\ell$ where $\Delta p, \Delta q$, and $\Delta\ell$ are invariant with p, q, and ℓ $U_Z'(x', y', z')$ may be written as

$$U_Z'(x', y', z') = \sum_p \sum_q \sum_\nu \sum_\eta f_{\nu\eta} \exp\left[-ik(p - \lambda\nu)k' - ik(q - \lambda\eta)y' - ik(\ell - \lambda\mu)(z' - Z) - ik\,\frac{\Delta p(p - \lambda\nu) + \Delta q(q - \lambda\eta)}{\left[1 - (p - \lambda\nu)^2 - (q - \lambda\eta)^2\right]^{1/2}}(z' - Z) - ik(\Delta p x' + \Delta q y')\right] \quad . \tag{45}$$

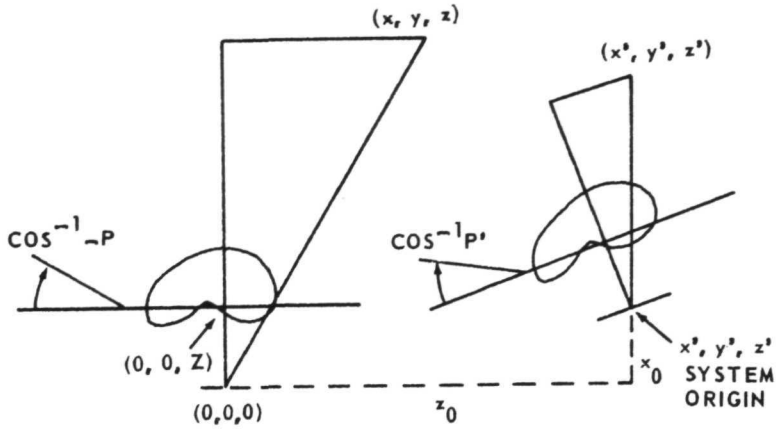

Figure 5. Image translation and rotation.

In equation (45) the term $\Delta\ell$ has been replaced by $(p - \lambda\nu)$ and $(q - \lambda\eta)$ because of the the wave equation relationship of equation (40). An examination of equation (45) reveals that the diffraction pattern at x', y', z' is identical to the diffractin pattern in equation (44) except for a small rotation about the $x', y', z' - Z$ origin. This rotation between the primed and double-primed systems may be described by the matrix

$$\begin{vmatrix} x'' \\ y'' \\ z'' \end{vmatrix} - \begin{vmatrix} 0 \\ 0 \\ Z \end{vmatrix} = \begin{vmatrix} 1 & 0 & \Lambda \\ 0 & 1 & \Omega \\ -\Lambda & -\Omega & 1 \end{vmatrix} \left[\begin{vmatrix} x' \\ y' \\ z' \end{vmatrix} - \begin{vmatrix} 0 \\ 0 \\ Z \end{vmatrix} \right] \tag{46}$$

where

$$\Lambda = \Delta p \left[1 - (p - \lambda\nu)^2 - (q - \lambda\eta)^2\right]^{-1/2} \tag{47}$$

and

$$\Omega = \Delta q \left[1 - (p - \lambda\nu)^2 - (q - \lambda\eta)^2\right]^{-1/2} . \tag{48}$$

This rotation is shown in Figure 6. This may be expressed in shorthand notation as

$$\left|X''\right| - \left|Z\right| = \left|\Lambda\right| \left[\left|X''\right| - \left|Z\right|\right] . \tag{49}$$

Thus equation (45) may be written as

$$U_Z(x'', y'', z'') = \sum_p \sum_q \sum_\nu \sum_\eta f_{\nu\eta} \exp\left[ik \sum_i j_i\right] \tag{50}$$

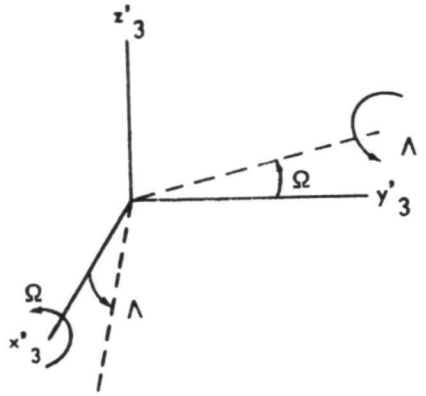

Figure 6. Equivalent rotation resulting from illumination.

where j_i is a general term in the matrix

$$\left| J \right| = \left| p - \lambda\nu \right|^T \left[\left| X'' \right| - \left| Z \right| \right] . \tag{51}$$

It appears then that a small rotation of the illuminating wavefront on a plane causes the diffraction pattern to be slightly rotated about the origin on the plane. This result is certainly what one would expect. Furthermore, the angles Λ and Ω can be related to the change in direction cosines of the illuminating wavefront, Δp and Δq, by equation (36)

$$\cos(\phi_x + \Lambda) = (p + \Delta p) - \lambda\nu \tag{52}$$

$$\Lambda \sin \phi_x = -\Delta p \quad . \tag{53}$$

A further rotation of the x', y', z' coordinates may be carried out to write equation (50) in terms of x, y, z. This rotation and translation is, of course, the Euler matrix of equation (7)

$$\left| X'' \right| = \left| E_{x'x} \right| \left[\left| x \right| - \left| T \right| \right] \quad .$$

The transformation for the terms in equation (50) is then

$$\left| J \right| = \left| p - \lambda\nu \right|^T \left| \Lambda \right| \left[\left| E_{x'x} \right| \left(\left| x \right| - \left| T \right| \right) - \left| Z \right| \right] \quad . \tag{54}$$

The geometry of the interfering diffraction patterns of equations (41) and (50) is shown in Figure 7. Suppose that some centroid of the diffraction pattern of interest makes an angle θ with the object grating and that the particular point of interest in the diffracted field is P. In the double-primed system, this same angle, θ, exists and the point in the diffracted field to be investigated is P''. If the two centroids intersect each

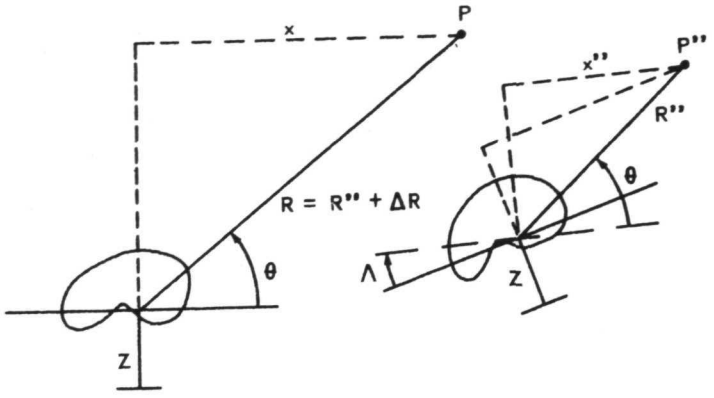

Figure 7. Diffraction patterns generating interference structure.

other, there is a possibility of fringe construction. This implies that somewhere, some point P must lie on P''. Fringes would certainly occur about P, in this case, if R were equal to R'', because two exactly similar diffracted fields would overlay each other at P with a difference only in their direction of propagation. But R is not in general equal to R'', and the wavefront from the original object travels a slightly different distance to P than does the wavefront from the displaced and rotated object. Since one is concerned with small displacement and rotations, this additional effect will be essentially approximate to a delay term designated by the extra distance ΔR. However, it is more exact to designate this extra delay distance not as ΔR, but as ΔL, where ΔL is the delay term accredited to each individual plane wave emanating from the object plane at the characteristic angle of ϕ. Recall that $\cos \phi_x = p - \lambda\nu$ for the x-directed component.

An approximation of ΔL may be carried out as follows, with the aid of Figure 8:

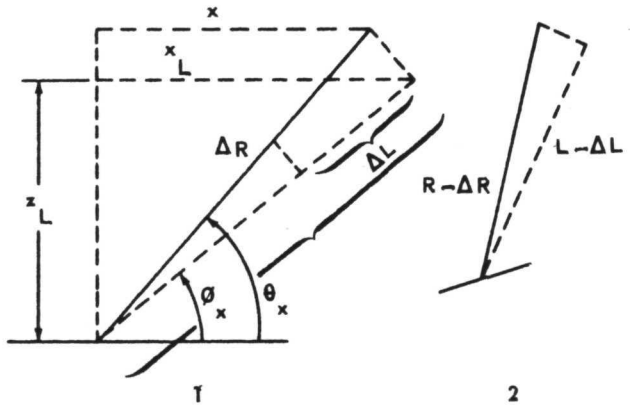

Figure 8. Range-difference (ΔR) geometry.

$$\Delta L = (p - \lambda\nu)\,\Delta L\ \frac{x_L}{L} + (q - \lambda\eta)\Delta L\ \frac{y_L}{L} + (\ell - \lambda\mu)\Delta L\ \frac{z_L}{L}$$

$$= (p - \lambda\nu)\Delta R\ \frac{x}{R} + (q - \lambda\eta)\Delta R\ \frac{y}{R} + (\ell - \lambda\mu)\Delta R\ \frac{z-Z}{R}$$

$$+ \frac{\Delta R}{R}\left[(p - \lambda\nu)x \sin(\theta_x - \phi_x) + (q - \lambda\eta)y \sin(\theta_y - \phi_y)\right.$$

$$\left. + (\ell - \lambda\mu)z \sin(\theta_z - \phi_z)\right] \qquad (55)$$

where the approximation

$$x_L = x \sin(\theta_x - \phi_x) + x \qquad (56)$$

has been used.

The angle over which the illumination is gathered is represented by $2(\theta_x - \phi_x)$ max. This angle is almost always very small and the terms containing the sines of these angles in the above equation may be dropped. This is the second approximation of the analysis, the first being that the translations and rotations are small.

What has just been stated means that as a prerequisite for fringe construction the diffraction pattern from the translated and rotated object must be

$$U_Z(x'', y'', z'') = \sum_p \sum_q \sum_\nu \sum_\eta f_{\nu\eta} \exp\left[-ik \sum h_j + ik\,\Delta L\right] \qquad (57)$$

at the point $P = P''$. With the aid of equation (55) this condition is

$$U_Z(x'', y'', z'') = \sum_p \sum_q \sum_\nu \sum_\eta f_{\nu\eta} \exp\left[-ik\left(1 - \frac{\Delta R}{R}\right)\sum_i h_i\right] \qquad (58)$$

using the matrix relationship of equation (54), equation (50) is

$$U_Z(x'', y'', z'')$$

$$= \sum_p \sum_q \sum_\nu \sum_\eta f_{\nu\eta} \exp \left\{ -ik(p + \lambda\nu) \left[(x - x_g) + (y - y_g)(-a - \gamma) + (z - z_g) + (\beta \sin\gamma + \Lambda) - \Lambda Z \right] \right.$$

$$- ik(q - \lambda\eta) \left[(x - \lambda_g)(a + \gamma) + (y - y_g) + (z - z_g) + (\Omega - \beta\cos\gamma) - \Omega Z \right]$$

$$\left. - ik(\ell - \lambda\mu) \left[(x - x_g)(\beta \sin a - \Lambda) + (y - y_g) + (\beta \cos a - \Omega) + z - z_g - Z \right] \right\} . \quad (59)$$

By judiciously rearranging terms, one can write

$$U_Z(x'', y'', z'') = \sum_p \sum_q f_{\nu\eta} \exp \left[-ik\left(1 - \frac{\Delta R}{R}\right) \sum_i h_i \right]$$

$$\exp \left[i(p - \lambda\nu)\, Rw_x + i(q - \lambda\eta)\, Rw_y + i(\ell - \lambda\mu)\, Rw_z \right] \quad (60)$$

where

$$\frac{Rw_x}{K} = x_g + (a + \gamma)(y - y_g) - (z - z_g)(\beta \sin\gamma + \Lambda) + \Lambda Z - \frac{\Delta R_x}{R} \quad (61)$$

$$\frac{Rw_y}{K} = -(x - x_g)(\alpha + \gamma) + y_g - (z - z_g)(\Omega - \beta \cos\gamma) - \Omega Z - \frac{\Delta R_y}{R} \qquad (62)$$

$$\frac{Rw_z}{K} = -(x - x_g)(\beta \sin\alpha - \Lambda) - (y - y_g)(\beta \cos\alpha - \Omega) + z_g - \frac{\Delta R_z}{R} \qquad (63)$$

Equation (60) then is identical to the condition required for fringe construction as that given by equation (62) except for the extra terms in w_x, w_y, and w_z. So far, little has been said about Λ and Ω other than that they are related to the change in the direction cosines of the illuminating wavefronts, Δp and Δq, as indicated in equation (53). It appears that Λ is not independent of the grating frequency term $p - \lambda\nu$. However, as assumed, the variation of $p - \lambda\nu$ about the central value $\cos\theta = x/R$ is small and the second-order term for Λ in equation (47) may be approximated as ΔR. This approxmation again assumes that the aperture used to examine the fringes is small, a valid approximation in most cases. Then

$$\Lambda = \frac{\Delta p}{|z - Z|} R \qquad (64)$$

and

$$\Omega = \frac{\Delta p}{|z - Z|} R \qquad (65)$$

Both Δp and Δq were evaluated in the previous case and are presented here in a slightly modified form to include Z.

$$\Delta p = \frac{1}{R_0}\left[x_g + y_g(\alpha - \gamma) - z_0 \beta \sin\gamma\right] - \frac{x_0\left[x_0(x_g + Z\Lambda) + y_0(y_g + Z\Omega) + (z_0 - Z) z_g\right]}{R_0^3} \qquad (66)$$

$$\Delta q = \frac{1}{R_0}\left[y_g - x_0(a+\gamma) + z_0\,\beta\cos\gamma\right]$$

$$- \frac{y_0\left[y_0(x_g + Z\Lambda) + y_0(y_g + Z\Omega) + (z_0 - Z)\,z_g\right]}{R_0^3} \quad . \tag{67}$$

and the source is assumed to be far from the object.

If equation (62) is a valid criterion for fringe formation, then w_x, w_y, and w_z should reduce to zero for perfect fringe construction. For fringes forming far off the object (more than 1000 wavelengths), these conditions should be identical to those arrived at by the analysis in the previous case. When the substitution is made for ΔR,

$$\Delta R = \frac{x(x_g + Z\Lambda) + y(y_g + Z\Omega) + (z - Z)\,z_g}{R} \quad . \tag{68}$$

Then the conditions for fringe formation are

$$\frac{x_g + (y - y_g)(a+\gamma) - (z - z_g)\,\beta\sin\gamma}{R} - \frac{x\left[x(x_g + Z\Lambda) + y(y_g + Z\Omega) + (z - Z)\,z_g\right]}{R^3}$$

$$= -\left\{\frac{x_g + y_0(a+\gamma) - z_0\,\beta\sin\gamma}{R_0} - \frac{x_0\left[x_0(x_g - Z\Lambda) + y_0(y_g + Z\Omega) + (z_0 - Z)\,z_g\right]}{R_0^3}\right\} \tag{69}$$

and

$$\frac{y_g - (x - x_g)(a+\gamma) + (z - z_g)\,\beta\cos\gamma}{R} - \frac{y\left[x(x_g + Z\Lambda) + y(y_g + Z\Omega) + (z - Z)\,z_g\right]}{R^3}$$

$$= -\left\{\frac{y_g - x_0(a+\gamma) + z_0\,\beta\cos\gamma}{R_0} - \frac{y_0\left[x_0(x_g + Z\Lambda) + y_0(y_g + Z\Omega) + (z_0 - Z)\,z_g\right]}{R_0^3}\right\} \tag{70}$$

and

$$\frac{z_g - (x - x_g)\,\beta \sin \alpha - (y - y_g)\,\beta \cos \gamma}{R} - \frac{z\left[x(x_g + Z\Lambda) + y(y_g + Z\Omega) + (z - Z)\,z_g\right]}{R_0^3}$$

$$= -\left\{\frac{z_g - x_0\,\beta \sin \alpha - y_0\,\beta \cos \alpha}{R_0} - \frac{z_0\left[(\lambda_0 + Z\Lambda) + y_0(y_g + Z\Omega) + (z_0 - Z)\,z_g\right]}{R_0^3}\right\} . \tag{71}$$

If the object point of interest lies at the origin, then $Z = 0$ and these equations are identical to equations (27), (28), and (29) if R is large.

Equation (71) is not arrived at directly from equation (59) but by the following manipulations of the wave-equation conditions of equation (40). A wave-equation relationship exists like that of equation (40)

$$(p + \Delta p - \lambda\nu)^2 + (q + \Delta q - \lambda\eta)^2 + (\ell + \Delta\ell - \lambda\mu)^2 = 1 . \tag{72}$$

This equation in conjunction with equation (40) gives

$$(p - \lambda\nu)\,\Delta p + (q - \lambda\eta)\,\Delta q + (\ell - \lambda\mu)\,\Delta\ell = -\Delta p^2 - \Delta q^2 - \Delta\ell^2 . \tag{73}$$

Since the angle over which the illumination is gathered is small, $p - \lambda\nu$ is approximately x/R. Dropping second-order terms in equation (73) gives

$$\frac{x}{R}\,\Delta p + \frac{y}{R}\,\Delta q + \frac{z}{R}\,\Delta\ell = 0 . \tag{74}$$

The function $\Delta\ell$ may be evaluated by investigating another condition on the wave equation.

$$(p + \Delta p)^2 + (q + \Delta q)^2 + (\ell + \Delta\ell)^2 = 1 . \tag{75}$$

Therefore,

$$\Delta p \cdot p + \Delta q \cdot q + \Delta \ell \cdot \ell = 0 \tag{76}$$

and

$$\Delta \ell = \frac{x_0}{z_0} \Delta p + \frac{y_0}{z_0} \Delta q \quad . \tag{77}$$

Using the previous equations for Δp and Δq gives

$$\Delta \ell = \frac{z_g - x_0 \beta \sin \alpha - y_0 \beta \cos \alpha}{R_0}$$

$$- \frac{z_0 \left[x_0 (x_g + Z\Lambda) + y_0 (y_g + Z\Omega) + (z_0 - Z) z_g \right]}{R_0^3} \quad . \tag{78}$$

The term

$$x\Lambda + y\Omega$$

in equation (63) is approximately

$$x \frac{R}{z} \Delta p + y \frac{R}{z} \Delta q$$

which is equal to $R\Delta \ell$ from equation (74). If $x\Lambda + y\Omega$ in equation (63) is replaced by $R\Delta \ell$ where $\Delta \ell$ is given by equation (78), the desired equation (71) results.

In summarizing the technique, the two wavefronts that interfere are given by equations (41) and (61). If fringes result from this interference, then the values of w_x, w_y, w_z of equations (61), (62), and (63) must equal zero. This condition reduces to the conditions of equations (69), (70), and (71) which reduce to equations (61), (62) and (63) for fringes far off the object. Fringes resulting from a point on the image and a similar point on the object occur whenever $R'' - R$ (Fig. 7) is some multiple number of wavelengths. The frequency of the resulting fringes in the x direction is then

$$\frac{1}{D_\lambda} = \frac{\partial \left[\frac{R'' - R}{\lambda} \right]}{\partial x} = \frac{x}{\lambda} \left[\frac{1}{R+\Delta R} - \frac{1}{R} \right] - \frac{x_g}{\lambda} \frac{1}{R + \Delta R} \quad . \tag{79}$$

Here again, if R is large, the fringe frequency corresponds to that of the previous case, for then

$$\frac{1}{D_x} = \frac{1}{\lambda} \left[\frac{x_g}{R} - \frac{x(xx_g + yy_g + zz_g)}{R^3} \right] \quad . \tag{80}$$

The distance $R'' - R$ is invariant to a transformation of coordinates, since transformation in an orthogonal system preserves vector lengths. We may write equation (80) as

$$\frac{1}{D_x} = \frac{x_g}{\lambda R_\ell} \tag{81}$$

where the coordinates are now aligned along the line-of-sight vector R_ℓ, and x_ℓ, x_g, y_ℓ, and y_g are normal to the line of sight. This is valid since we have not chosen the direction of orientation for our coordinate system in the preceding analysis. This is, in fact, the usual way the fringes are observed, lateral to the line of sight that passes through the fringes to the object. Similarly, in the y direction lateral to the line of sight, we have

$$\frac{1}{D_y} = \frac{y_g}{\lambda R_\ell} \tag{82}$$

while the z-direction term along the line of sight results in $D_z = 0$. To find all three translations, x_g, y_g, and z_g, and thus relate them to the original coordinate system, it is necessary to examine the fringe structure from two different line-of-sight angles; i.e., two different combinations of θ_x and θ_y.

Once all three translations have been found, the rotations α, β, and γ may be determined from equations (69), (70), and (71). Equations (64) through (67) are required to solve for Λ and Ω. However, R_0 is usually large enough that the z terms of equations (66), (67), and (78) may be neglected, which simplifies the equations.

III. EXPERIMENTAL SYSTEM

Two experimental setups were used in this effort. Figure 9 shows the first system used. This setup utilized a 50-mW HeNe laser and a 40.64-cm diameter concave mirror as the test object. Finer mirror adjustments and shorter exposure times were desired so the setup shown in Figure 10 was used. In this system, an argon laser was used along with 20.32-cm-diameter schlieren mirrors which had fine adjustments about two axes. Figures 11 and 12 are photographs of the optical component layout for this system which produced the data discussed in the next section of this report.

The reference beam used was a collimated 10.16-cm diameter beam. The test mirror was illuminated by a 30.48-cm-diameter diffuser so that, upon reconstruction, the fringes appear on a soft illuminated background. A precision plateholder with x-y adjustment and a liquid gate was used to hold the film plate so that real-time analysis could be achieved. Real-time analysis was conducted, but for ease of presentation, only data from double-exposed holograms will be discussed. They essentially represent individual frames from the continuous real-time observations. The entire system, with the exception of the laser, is supported by a 1.22- by 1.83-meter granite slab resting on air mounts. This provided an extremely stable platform for the holometer so long-term inspections could be made.

IV. EXPERIMENTAL RESULTS

Since most of this effort utilized the holometer with the argon laser (Fig. 10), data from that phase of the effort will be discussed. A 20.32-cm diameter schlieren mirror that is flat to 1/8 wavelength was used as the test mirror. Using the 4880-A line from the laser and Agfa Gaveart 10E56 photographic plates, the total exposure times were ~ 0.3 second.

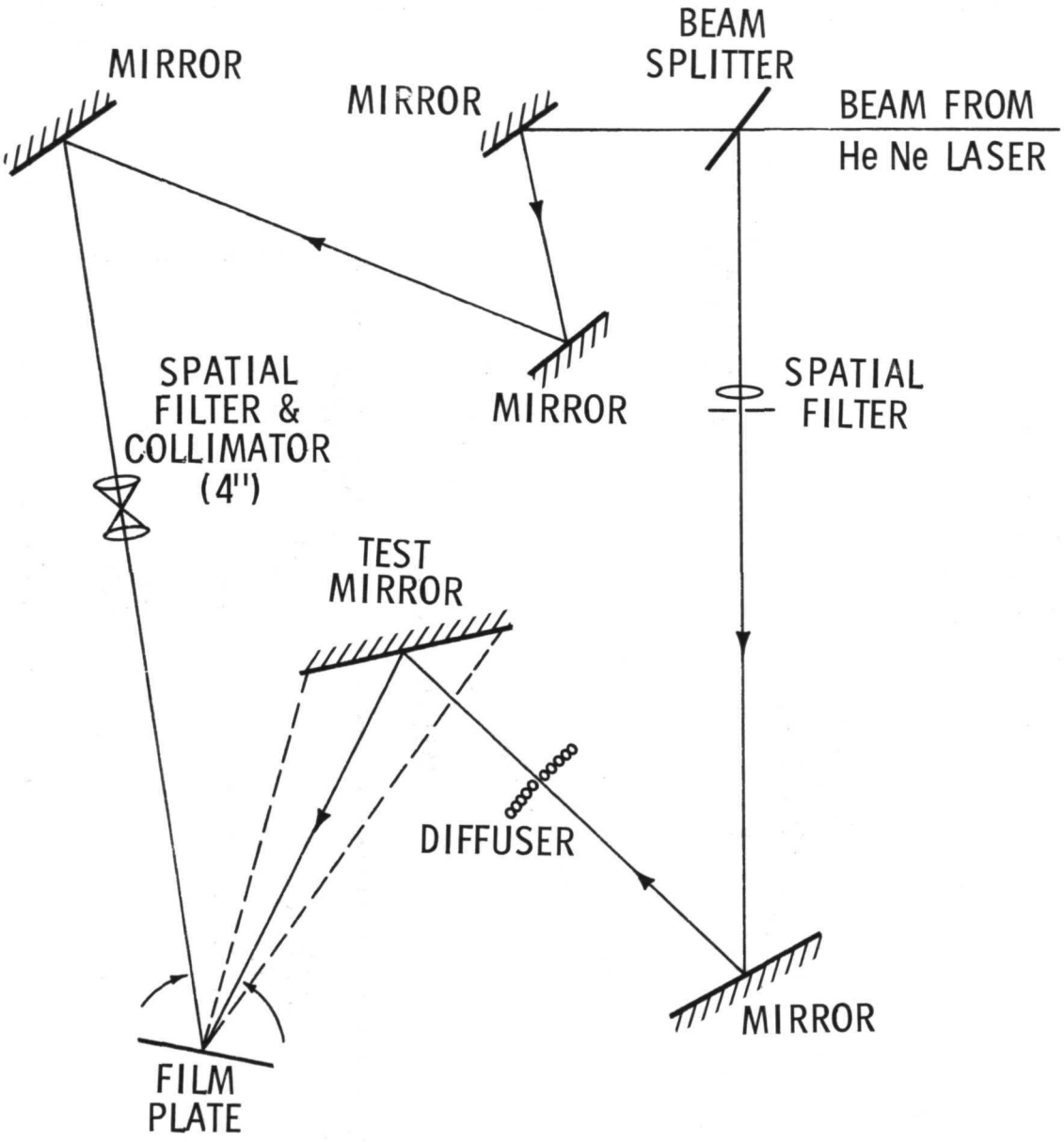

Figure 9. Optical component holometer (holographic interferometer).

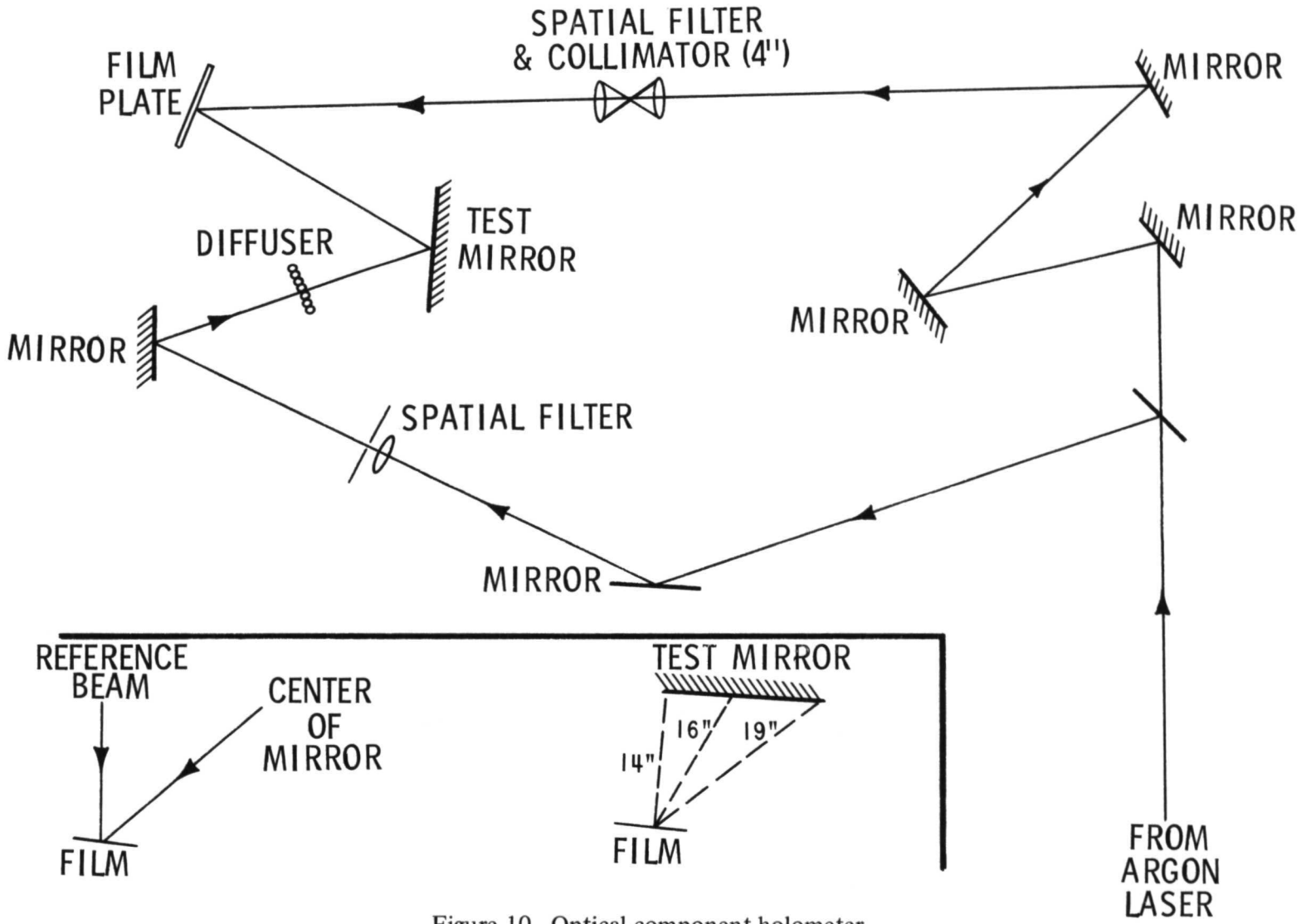

Figure 10. Optical component holometer.

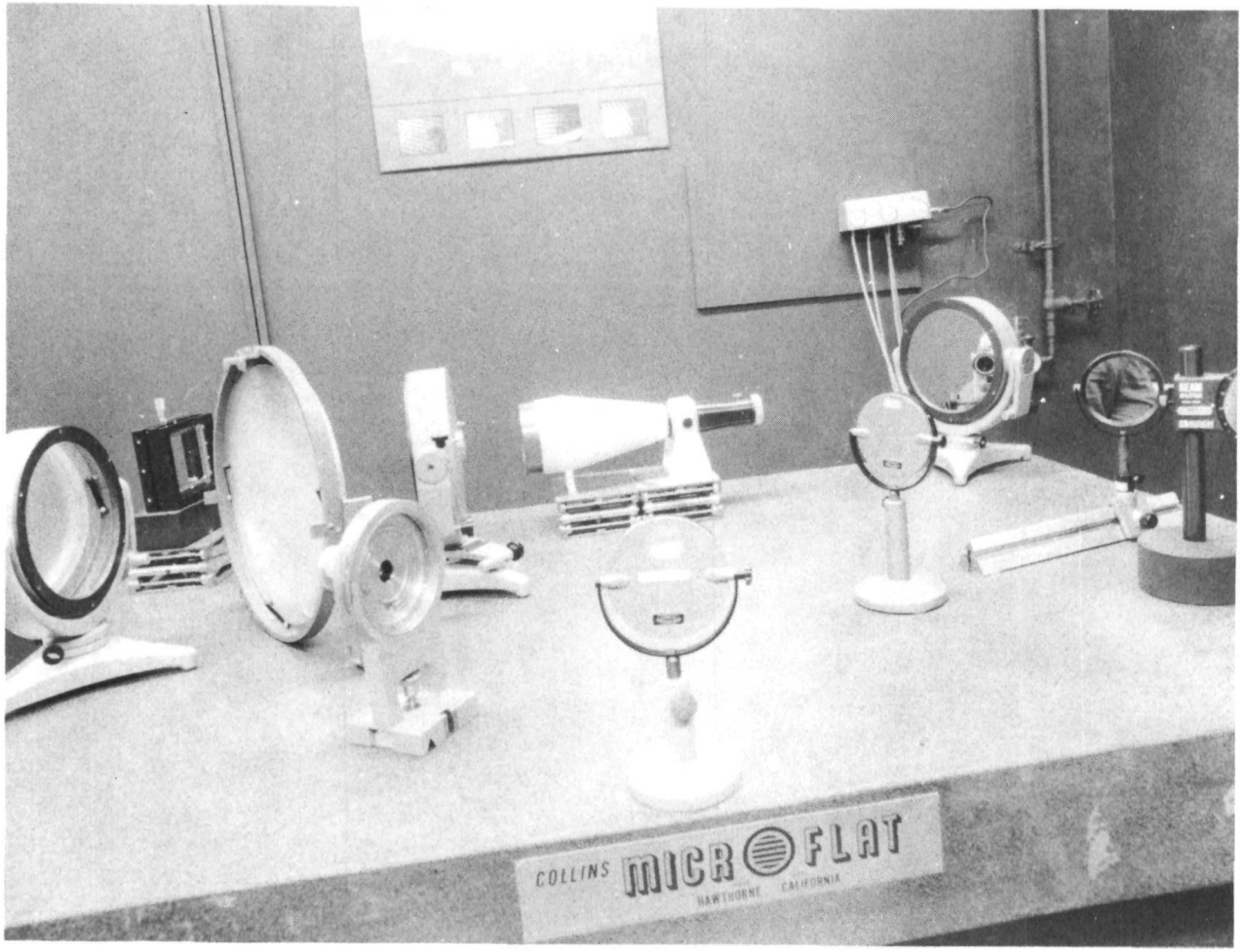

Figure 11. Experimental holographic interferometer.

Figure 12. Experimental holographic interferometer.

The data presented in this section were extracted from the real image of double-exposed holograms. The test mirror was rotated about the vertical axis between exposures. At various intervals in the testing period, double-exposed holograms were made with no mirror rotation. The time between exposures for these holograms was ~ 10 minutes so they were used as controls to determine whether any component shifting or mode oscillation in the laser would add or subtract any information contained in the fringe structure of the hologram. Only one hologram, very early in this effort, displayed component instability and this was evident by a "washing out" of ~ 40 percent of the holographic image upon reconstruction. All subsequent tests have produced very bright reconstructions, and the fringes formed by rotation of the surface were either on the surface or a very small distance (few wavelengths) from the surface. Under this condition, all calculations follow from Section II, Case 1, of this report. Three cases with different magnitudes of rotation are as follows.

Case 1 represents a fringe spacing, D, of 1.854 cm. To obtain an accurate measurement of this fringe spacing, all measurements were takn in the same plane as the original object appeared. This plane is shown in Figure 13. From these measurements, the angle, α, of rotation of the surface was computed. For a β of 73.8 degrees, α for this case is 7.677×10^{-4} degrees or 2.764 seconds of arc. From this angle, the change in displacement, ΔL, for any point along the movement axis of the mirror can be calculated. Figure 14 is a plot of ΔL versus the distance from the center of rotation.

Case 2 represents a fringe spacing of 0.942 cm. The measurements and calculations are the same as in Case 1. For a β of 73.8 degrees, α is 1.513×10^{-3} degrees or 5.447 seconds of arc. Figure 15 shows the reconstructed fringes while Figure 16 shows ΔL versus distance from the center of rotation.

Case 3 represents a fringe spacing of 0.724 cm. The measurements are again the same as in Case 1. For a β of 73.8 degrees, α is 1.971×10^{-3} degrees or 7.096 seconds of arc. Figure 17 shows the reconstructed fringes while Figure 18 shows ΔL versus the distance from the center of rotation.

V. CONCLUSIONS

The "quick look" described in this report generated useful data and indications as to the applicability of holographic interferometry to the testing and monitoring of large mirrors. We are able to detect and measure the change in an optical surface caused by rotation. Even though this is the simplest case, it indicates the sensitivity of such a device. The extension of this effort to x, y, z translations and various combinations thereof will produce a more complete picture of its applicability.

George C. Marshall Space Flight Center
National Aeronautics and Space Administration
Marshall Space Flight Center, Alabama 35812, August 13, 1970
981-10-10-00-62

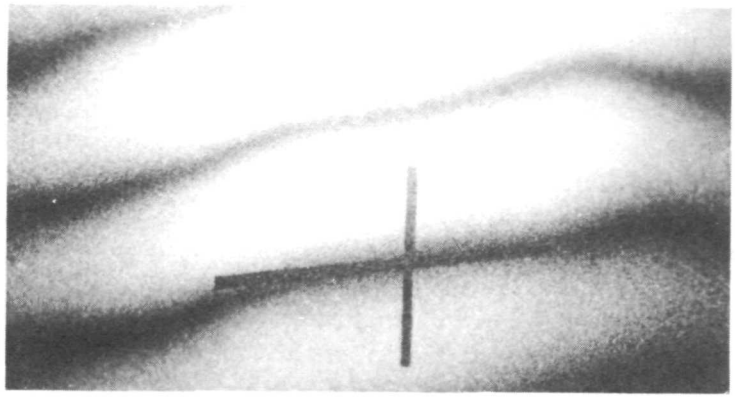

Figure 13. Reconstructed holographic fringes for Case 1.

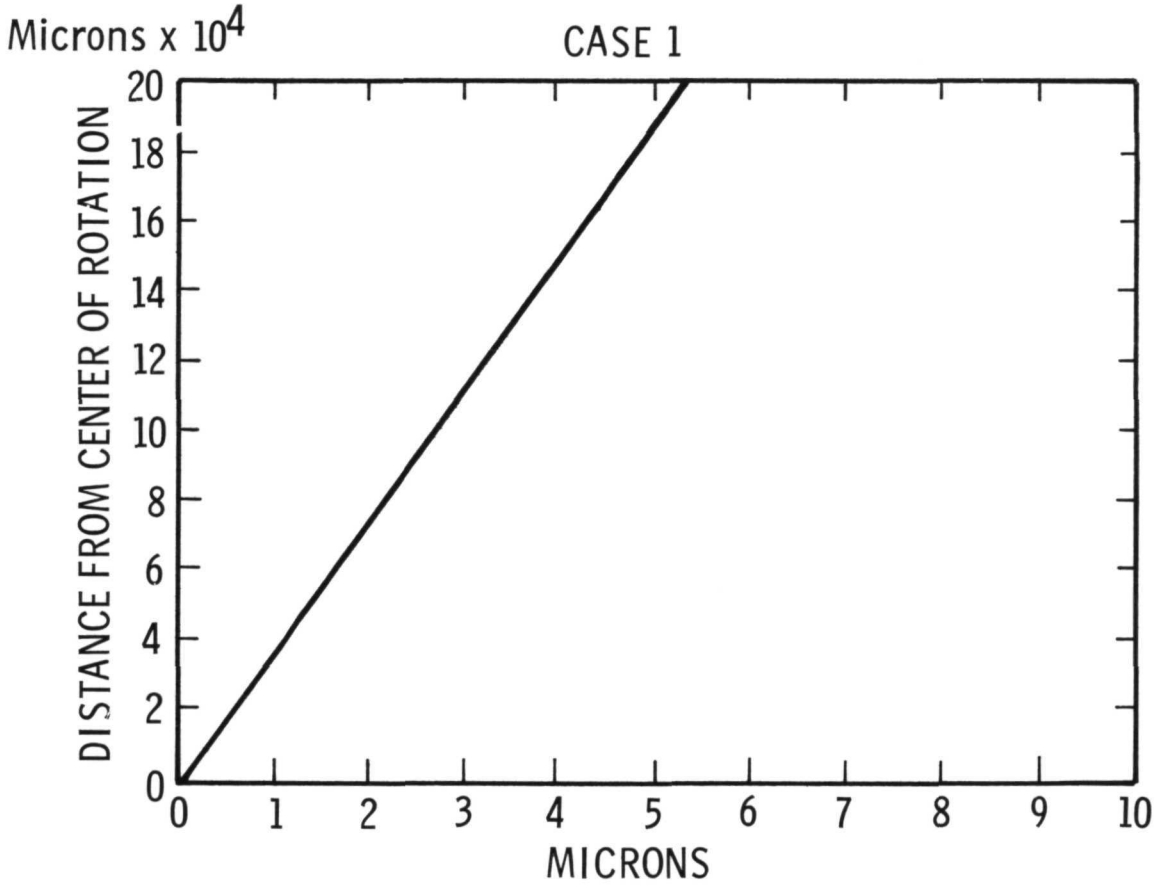

Figure 14. ΔL versus the distance from the center of rotation.

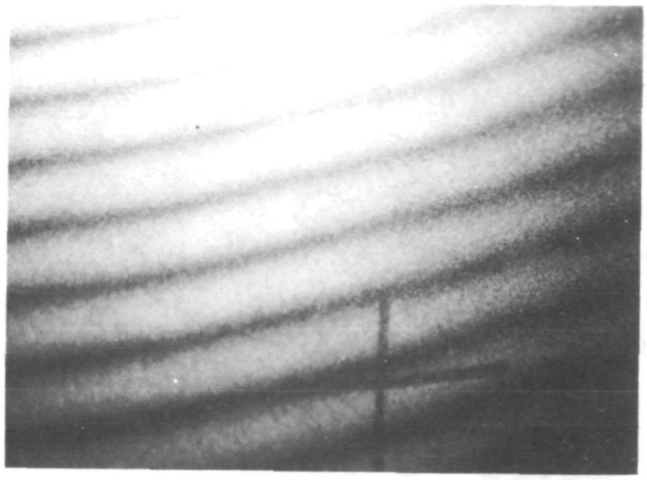

Figure 15. Reconstructed holographic fringes for Case 2.

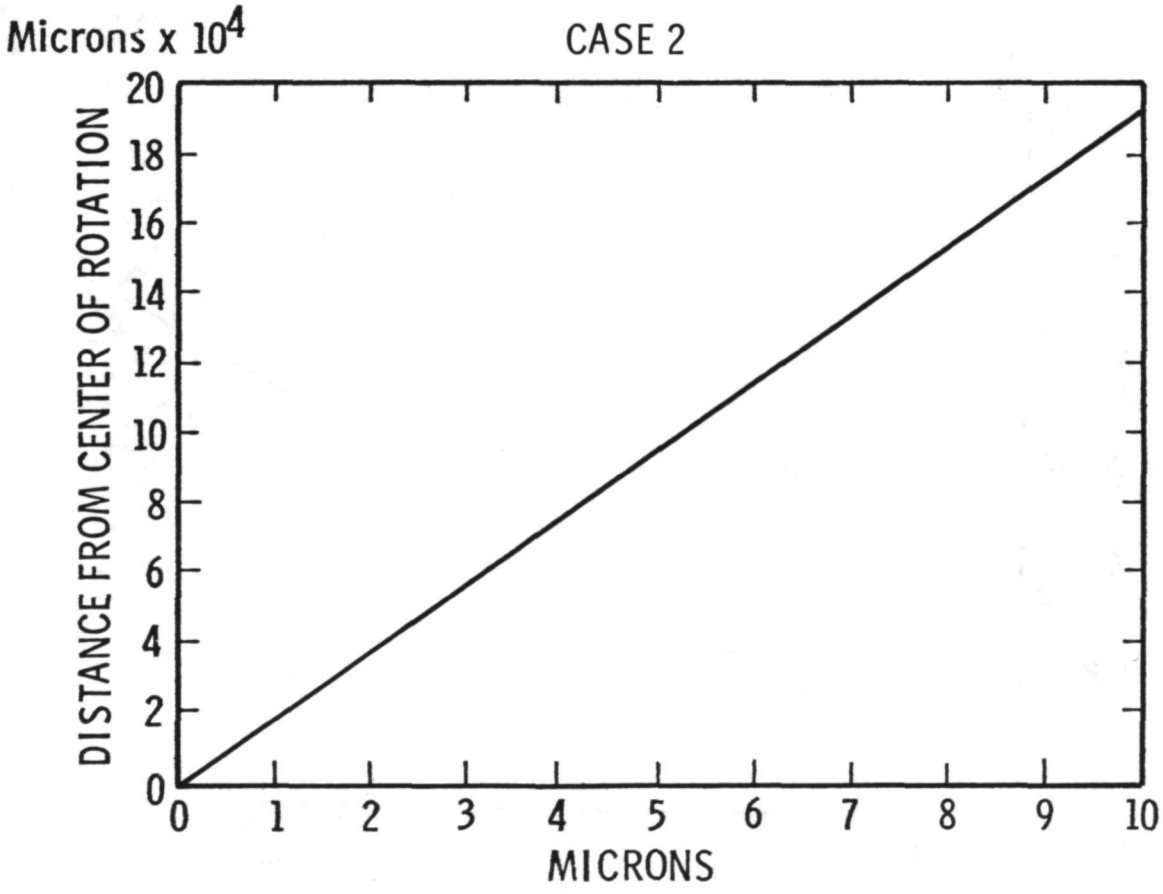

Figure 16. ΔL versus the distance from the center of rotation.

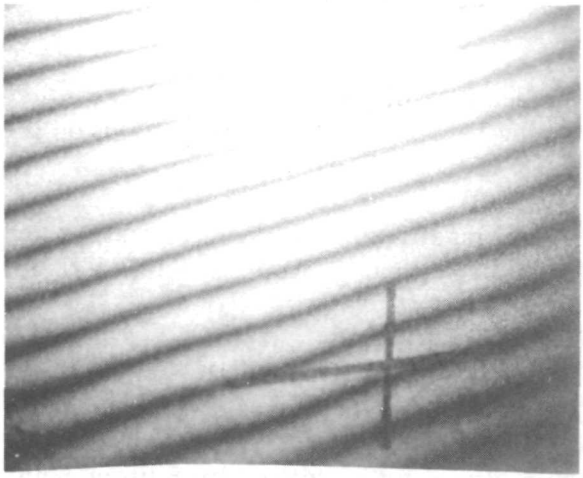

Figure 17. Reconstructed holographic fringes for Case 3.

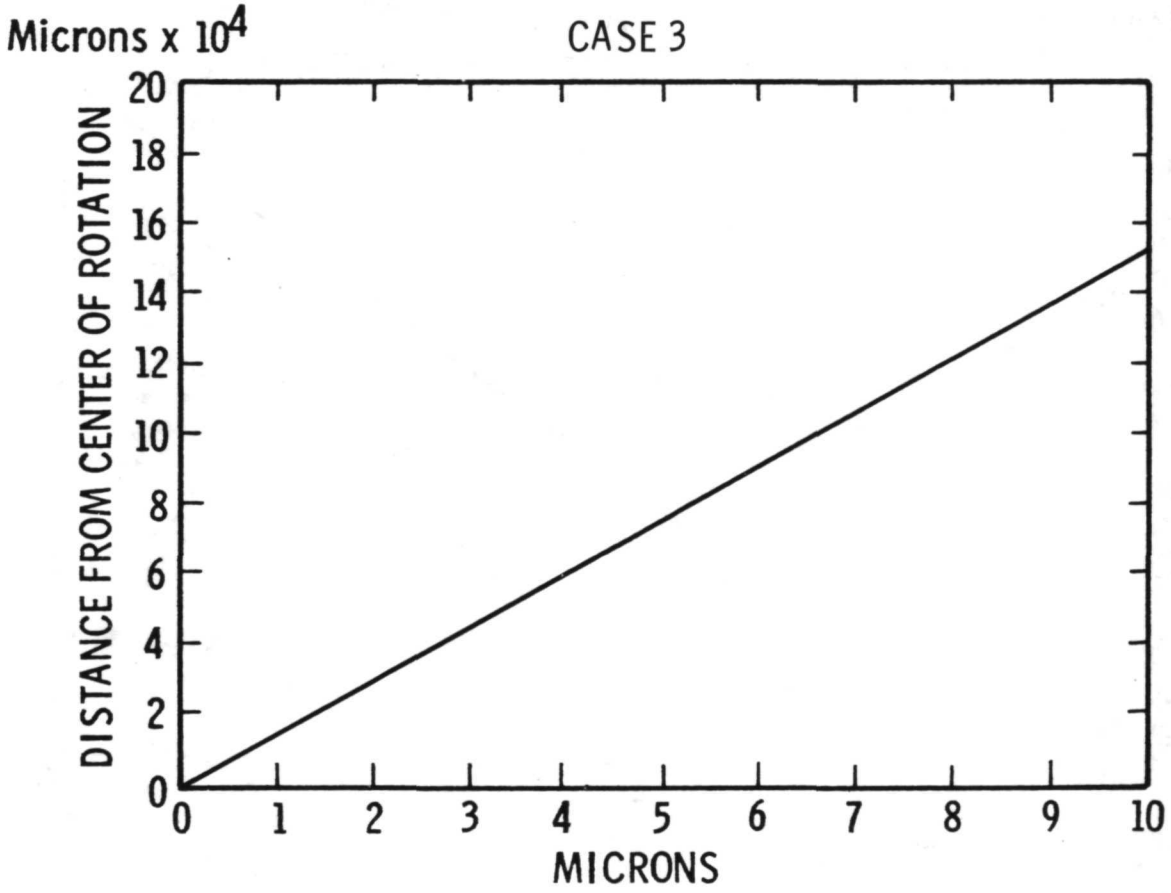

Figure 18. ΔL versus the distance from the center of rotation.

REFERENCES

1. Haines, K. A., and Hildebrand, B. P.: Interferometric Measurements on Diffuse Surfaces by Holographic Techniques. IEEE Transactions on Instrumentation and Measurements, Vol. 1N-15, No. 4, December 1966.

2. Haines, K. A., and Hildebrand, B. P.: Surface-Deformation Measurement Using the Wavefront Reconstruction Technique. Applied Optics, Vol. 5, No. 4, April 1966.

BIBLIOGRAPHY

Born, Max, and Wolf, Emil: Principles of Optics. 3rd Edition, Pergamon Press, New York, 1965.

Francon, M.: Optical Interferometry. Academic Press, New York, 1966.

Goodman, J. W.: Introduction to Fourier Optics. McGraw-Hill, New York, 1968.

Hildebrand, B. P., and Haines, K. A.: Holography as a Tool in the Testing of Large Aperture Optics. Applied Optics, Vol. 6, No. 7, July 1967.

NASA-Langley, 1971 —— 16 M437